Journal of Engineering Science and Technology
Special Issue on SU18, February (2019) 168 - 178

BASIC CHARACTERISTICS OF WIRELESS POWER TRANSFER

F. AZHAR[1,*], N. A. MOHD NASIR[1],
A. L. HAKIM[1], R. N. FIRDAUS[1], ARAVIND C. V.[2]

[1]Faculty of Electrical Engineering, Universiti Teknikal Malaysia Melaka,
Hang Tuah Jaya, Durian Tunggal, Melaka 76100, Malaysia
[2]School of Engineering, Taylor's University, Taylor's Lakeside Campus,
No. 1 Jalan Taylor's, 47500, Subang Jaya, Selangor Darul Ehsan, Malaysia
*Corresponding Author: fairul.azhar@utem.edu.my

Abstract

Nowadays, wireless power transfer had been used in many applications such as the mobile phone and Electric Vehicle (EV) charging. This paper presented an idea that is discussed a concept of wireless power transfer. The basic design, merits, and demerits, applications of wireless power transfer are also discussed. Through laboratory experiment testing, data is collected and analysed. Construction of a prototype and the complete schematic of the prototype is presented in this paper. The performance of the WPT is analysed. The experiment starting with the hardware fabrication of the WPT module and the single-phase inverter. By proceeding with measurement of a characteristic of the WPT, which are the resistance (R), inductance (L), voltages (V) current (I) and power (P); some experiments were done to get expected results, which meet the objectives of the project.

Keywords: Single-phase inverter, Wireless power transfer.

1. Introduction

Wireless Power Transfer (WPT) is the transmission of supply power to an electrical load through an air gap without the need of current carrying conductor such as cables and wires [1]. WPT has been recognized to improve convenience and reliability of application such as transportation. Chopra and Bauer [2] and Qiu et al. [3] explained, besides transportation like Electric Vehicles (EV), WPT technology is widely used throughout the world and applied to various applications such as mobile phones, laptops, and biomedical implant [4].

In general, WPT transfer power from Direct Current (DC) supply then converted to Alternative Current (AC). The wireless power involves the transmission of energy from a transmitter to a receiver via an oscillating magnetic field. WPT uses fields created by charging particles to carry energy between transmitters and receivers over an air gap. The air gap is bridged by converting the energy into a form that can travel through the air.

Electric Vehicles (EV) charging is another application of the WPT. Recharging the battery for EV are demanded to be more reliable and convenient proportionally to the wide growth of the EV market. The charging of the battery requires no physical contact between the charging device and the vehicle according to the WPT concept.

2. Basic Concept of WPT

Wireless power transfer is the transmission of energy covering a distance without using wire or cable, which can be short or long distance. Wireless operations permit services, for example, long-distance communication, a purely unfeasible using wires. Wireless energy transfer or wireless power transmission can be a transfer of power from the hand's source to an electrical load without interconnecting wires. The most common form of wireless power transmission is ready to use direct induction and magnetic induction and resonant. Other methods under consideration include radio waves, such as microwaves or beam light technology. Wireless communication is mostly regarded as a branch of telecommunications. Wireless operations permit services, for example, long-range communication can be impossible and impractical in the conventional method.

2.1. Basic concept of WPT module

The module of the WPT consists of the primary coil, N_p and the secondary coil, N_s where N_s is larger than N_p in term of turns to produce output as higher as possible. The primary side of the coil is connected to the power source while the output is connected to the secondary side. The difference in voltage between the primary and the secondary windings is achieved by changing the number of coils turns in the primary winding N_p, compared to the number of coils turns on the secondary winding, N_s.

A ratio exists between the numbers of the turn of the primary coil isolated by the number of turns of the secondary coil. The turn ratio esteem directs the operation of the WPT and the output voltage accessible on the secondary coil. It is important to know the proportion of the ratio of turns of the coil on the primary and secondary. The turn proportion can be varied, for example, 1:3 (1-3). At that point, we can see that if the proportion between the numbers of turns changes the

production of the output voltage to prove Eq. (1), where V_p and V_s are primary voltage and secondary voltage correspondingly, as well as N_p and N_s, represents primary and secondary turn respectively.

However, the strength of the magnetic field induced in the coils depending on the amount of current and number of turns in the coil. When the current is reduced, the strength of the magnetic field also reduced. When the magnetic flux flows around the core, they pass through the secondary winding turns, causing the voltage to be induced in the secondary coil. The number of induced voltage will be determined by Eqs. (2) and (3), where V_p and V_s are primary voltage and secondary voltage respectively, N_p and N_s represent primary and secondary turn individually, and Ø is the flux between air gap.

This show that the same voltage is induced in each turn coil windings is both the same as the magnetic flux linking winding two windings together. As a result, the voltage induced in each winding is directly proportional to the number of turns of the coil. Besides increasing the number of turns of the coil in the primary winding, high magnetic field strength can be produced by increasing the current flow through the coil.

$$\frac{N_p}{N_s} = \frac{V_p}{V_s} \tag{1}$$

$$V_p = N_p \frac{d\emptyset}{dt} \tag{2}$$

$$V_s = N_s \frac{d\emptyset}{dt} \tag{3}$$

2.2. Basic concept of inverter

Phogat [5] reported that the inverter used in this project is a single-phase inverter. The purpose of the DC-AC inverter is to take DC power from a battery source and converts it to AC. Inverters are used for a variety of applications that range from small car adapters to household or office applications, and large grid systems. The basic circuits include an oscillator, control circuit, a drive circuit for the power devices, switching devices, and a transformer. The conversion of direct to alternating voltage is achieved by converting energy stored in the DC source such as the battery, or from a rectifier output, into an alternating voltage. This is done using switching devices, which are continuously turned on and off, and then stepping up using the transformer. Although there are some configurations, which do not use a transformer are not widely used. The DC input voltage is switched on and off by the power devices such as MOSFETs or power transistor. The switching elements nowadays such as Bipolar Junction Transistor (BJT), Gate Turn Off Thyristor (GTO), an Insulated Gate Bipolar Transistor (IGBT) can also be used as a switch. According to Ismail et al. [6], Vujacic et al. [7] and Gopinath [8], there are substituting the relays, magnetic switches and other magnetic components as the inverter switching devices.

3. Construction and Experiment of Wireless Power Transfer

The construction of the WPT involves constructing the WPT module and the single-phase inverter. The project then proceeds with the characteristics measurement. There are two main experiments involves in conducting this project, which are the measurements of R-L characteristics and the measurements

of performance characteristics. The parameters of performance characteristics are voltage (V), current (I) and power (P). From the power characteristics, the efficiency are calculated.

3.1. Construction of WPT module

Figure 1 shows the structure of the WPT module. The module consists of 2 cores, which are the C-core and the I-core. These two cores are designed for induction of the voltage between the two windings by providing a path for the magnetic field. The module also has 2 windings, which are also known as coils, the primary coil, and the secondary coil. The primary winding is the coil that draws power from the sources. The secondary winding is the coil that delivers the energy or changed voltage to the load. Each coil has a different parameter in term of size, layers, and turns. The coil size of the primary coil is 0.9 mm that wrap around for 3 layers while the secondary coil size is 0.7 mm with 5 layers. Therefore, the turns of the primary coil, N_p is 127 turns while the turns of the secondary coil, N_s is 310 turns. The number of N_p is less than N_s as it's required to produce a higher voltage as possible. Various sizes of the slab are also used, which act as an air gap, δ between the two cores. The gaps, δ lengths are 1 mm, 2 mm, 3 mm, 4 mm, and 5 mm. The summarization of parameters of the coils is shown as in Table 1.

Table 1. Parameters of primary coil and secondary coil.

	Primary coil	Secondary coil
Number of turns	127	310
Copper size	0.9	0.7
Number of layer	3	5

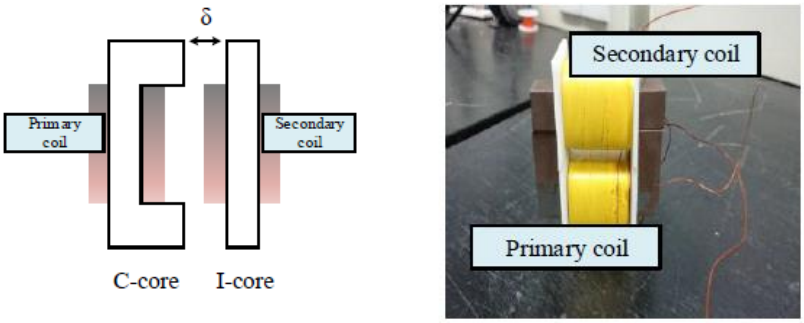

(a) Geometrical structure. **(b) Contructed structure.**

Fig. 1. Structure of WPT module.

3.2. Construction of single-phase inverter

To further the study of the WPT module, a single-phase inverter was constructed. The schematic diagram of the inverter circuit was firstly has been drawn using the PROTEUS software. After that, the inverter is ready to be constructed according to the schematic as in Fig. 2(b). All of the components were soldered to a circuit board and the connection was checked. The construction was using a wire-wrap method that can be modified afterwards.

Figure 2(b) shows the schematic circuit of the single-phase inverter. The inverter circuit was drawn accordingly and consist of components that been set to their parameters. The H-bridge circuits are used to construct the single-phase inverter. The IRF 640 act as MOSFET for the switching of the circuit powered by 15 V DC input to trigger the MOSFET. The MOSFET driver used is IR2110 in the H-bridge circuit. The input voltage supply is connected to terminal block J3. Terminal block J1 act as an input to the circuit while terminal block J2 as the output of the circuit.

As shown in Fig. 2(a), the inverter has two legs, left and right. Each leg consists of two switches connected in series. The H-bridge circuit consists of four switches corresponding to S1, S2, S3, and S4. There are four possible switch positions that can be used to obtain voltages across the load. These positions are outlined in Table 2. Note that all other possibilities are omitted, as they would short circuit power to the ground, potentially causing damage to the device or rapidly depleting the power supply.

Table 2. H-bridge switching state.

Voltage across load	S_1	S_2	S_3	S_4
Positive	On	On	Off	Off
Negative	Off	Off	On	On
Zero potential	On	Off	On	Off
Zero potential	Off	On	Off	On

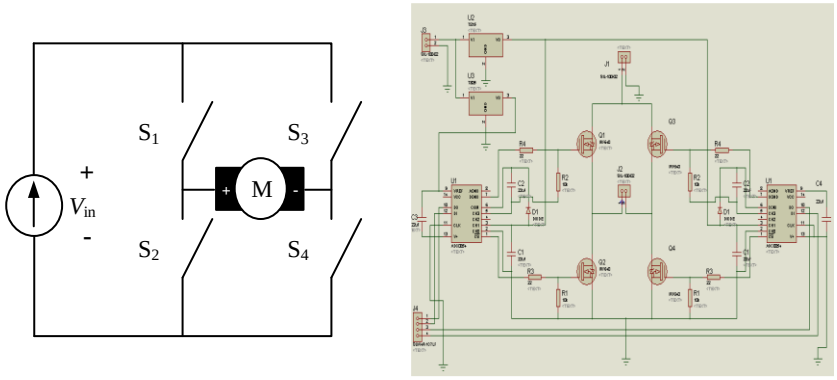

(a) H-bridge structure. **(b) Schematic diagram.**

Fig. 2. Single-phase inverter structure.

3.3. Characteristics measurement

For the R-L characteristics measurements, the measurement is aided with GW Instek LCR-819, LCR meter. The LCR meter is a type of electronic test equipment used to measure the inductance (L), capacitance (C), and resistance (R) of an electronic component. The RCL meter was connected to the primary coil and a secondary coil as in Fig. 3. The initial measurement is set with no air gap (0 mm) between the 2 cores. The LCR meter was connected to N_p with an initial frequency of 12 Hz that was set on the meter. The value of R and L was measured linearly

with the frequency as it increases to a max of 100 kHz. After that, the LCR meter was connected to N_s and the R and L were measured according to the frequency of 12 Hz to 100 kHz. The step was repeated by using a slab with different length act as an air gap between the cores. The measurement is continued with a gap of 1 mm, 2 mm, 3 mm, 4 mm, and 5 mm.

For the performance's characteristic measurement, the WPT module is connected with the single-phase inverter. Figure 4 shows the connection between the loaded experiment. The setup was generated by a 15 V DC source. The single-phase inverter was connected to the DC source and the microcontroller that was programmed from the laptop. The output of the inverter was connected to the primary coil of the WPT module. The experimental setup was shown in Fig. 4(b).

The measurement begins with no gap (0 mm) with the frequency of the inverter is set to 12 Hz. The measurement of voltage and current can be obtained where the input voltage, V_p and the input current, I_p are at the primary coil while the output voltage, V_s and the output current, I_s are at secondary coil. From the value of the current and voltage, the input power, $P_{p,}$ and output power, P_s can be calculated. The following parameters are measured by the frequency is increased to 24 kHz. The steps and measurements are repeated using a different air gap, 1 mm, 2 mm, 3 mm, 4 mm, and 5 mm, same as R-L characteristic experiment.

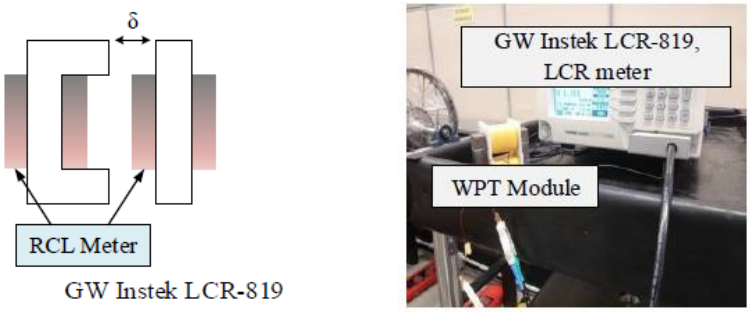

(a) Connection of coil with LRC meter **(b) Experiment setup of coil with LRC meter.**

Fig. 3. WPT module R-L characteristic experimental setup.

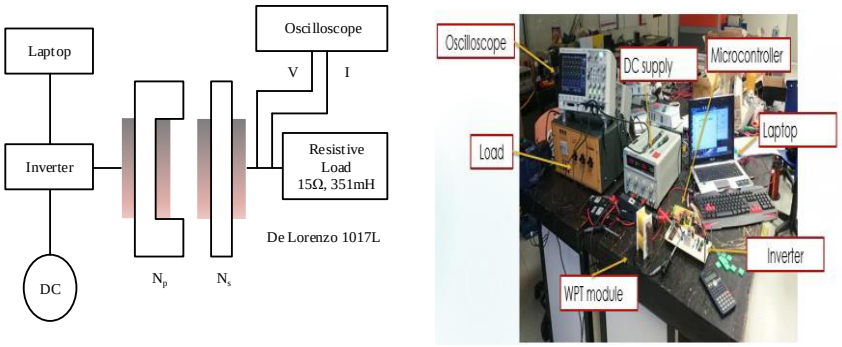

(a) Geometrical structure. **(b) Constructed structure.**

Fig. 4. WPT module performances characteristic experimental setup.

4. Basic Characteristics of Wireless Power Transfer

The fabricated WPT module was completed and the measurements results such as R-L characteristics, and the performance characteristics such as voltages (V), current (I) and power (P) are observed and tabulated. The measured characteristics are then presented in terms of graphs. The results of voltages (V), current (I), power (P), and efficiency are focused for on-load operations.

4.1. R-L characteristics

The R-L characteristics were observed at a range of frequency between 12 Hz to 100 kHz. The results of R-L characteristics are focused on the highest gap, which is 5 mm. The results of the R-L characteristic for the primary coil and the secondary coil are shown in Fig. 5. Generally, the results show a decreasing value of inductance with both the primary coil and secondary coil. The resistance and inductance measurements are higher with no gap and the values are slightly decreasing as the gap are increasing. The inductance of the coils decreases when a higher frequency is applied.

The value of inductance on the primary coil is decreasing and can be close to 0.4 mH as the minimum value at the maximum frequency of 100 kHz, whereas the minimum value of inductance is 1.9 mH on the secondary coil. The results also show that the resistance value increases as the frequency increase. The value of the resistance on the primary coil can reach a maximum of 71 Ω. On the secondary coil, the max resistance is 409 Ω when the max frequency of 100 kHz is applied. The resistance value on the secondary coil is higher than the primary coil. From the graph, the relationship between the resistance and inductance with frequency is the inversely proportional as the inductance will decrease while the resistance increase.

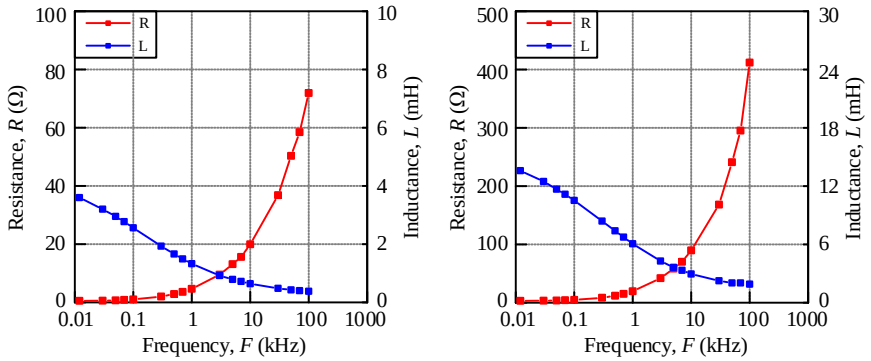

(a) Primary coil, N_p **(b) Secondary coil, N_s**

Fig. 5. R-L characteristics at 5 mm gap.

4.2. On-load voltage

Figure 6 shows the on-load voltage taken at gap 0 mm. The result waveforms show that the primary voltage, V_p mostly formed a square wave while the secondary voltage, V_s formed a triangle waveform. The secondary voltage, V_s has the highest

peak voltage of 6.9 V than the primary voltage, V_p on no gap as shown in Fig. 6(a). Throughout the experiments, it shows that the secondary voltage, V_s is lower than the input voltage when the gap increase. It clearly shows that the primary voltage, V_p mostly in a steady state as the frequency increase, however, the secondary voltage, V_s will decrease to under 1 V as the frequency increase. The input voltage of all the gaps tends to be steady while the decreasing of the output voltage is affected by the increase of the frequency and the gaps. The high input voltage in load condition is 5.7 V. Generally, secondary voltage, V_s is lower than primary voltage, V_p through the increasing of frequency almost to 1 kHz.

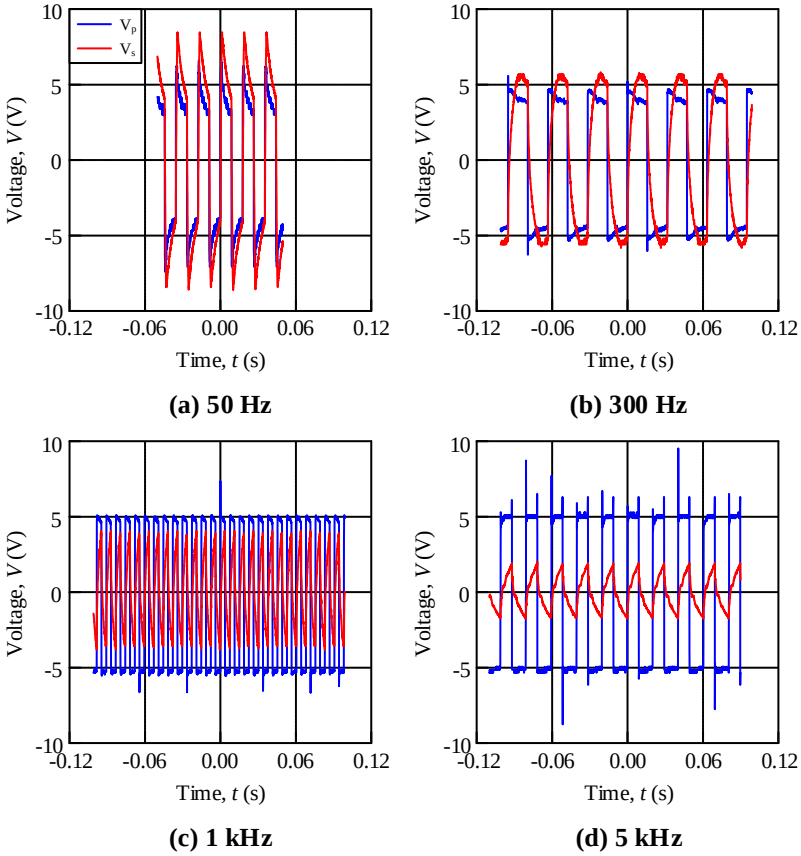

(a) 50 Hz **(b) 300 Hz**

(c) 1 kHz **(d) 5 kHz**

Fig. 6. On-load voltage characteristics.

4.3. On-load current

Figure 7 shows the waveforms of primary current, I_p and secondary current, I_s. The results are taken at a gap of 0 mm where both waveforms of primary current, I_p and secondary current, I_s obtained is in triangle waveform. The current characteristic shows that both of the primary current, I_p, and the output current decreasing as the frequency increase. The input current, I_p decreases almost to 0.5 mA while the output current, I_s decreasing and remain steady at 0.26 mA.

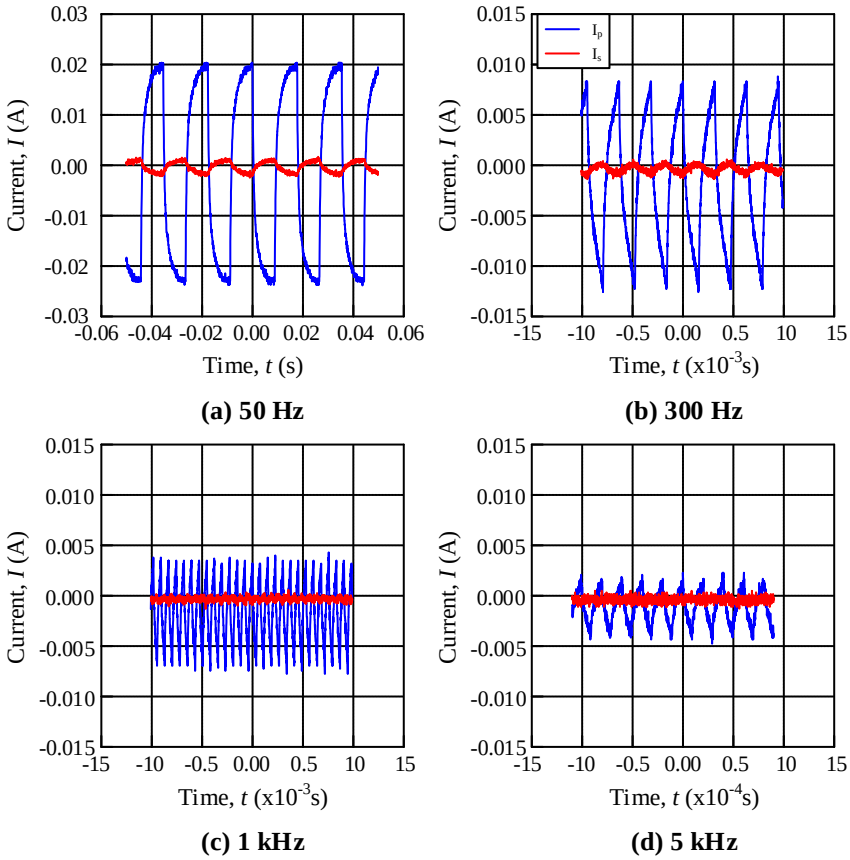

Fig. 7. On-load current characteristics.

4.4. Power

Figure 8 shows the results of power characteristics. The input power, P_{in} and the output power, P_{out} is calculated and plotted using the OriginLab software. The input power, P_{in} is decreasing as the gap increase from 0 mm to 5 mm where the highest input power, P_{in} captured is 103 W at 30 Hz for gap 0 mm. The same pattern of decreasing is shown by the output power, P_{out} where the highest output power, P_{out} produced is 8 W at 30 Hz for gap 0 mm. In general, the input power, P_{in} initially increasing up to 90 W, however then, decrease eventually as the frequency increase. This can also be seen on the output power, P_{out}. The output power, P_{out} is decreasing greatly as the gaps increase.

Based on the performances of input power and output power, the efficiency is calculated by using Eq. (4) where η is efficiency, P_{out} is output power in watt and P_{in} input power in watt. The graph in Fig. 8 shows that the efficiency decreases as the gap increase. The efficiency of the gap 0 mm is dropped to almost 0.01% at gap 5 mm.

$$\eta = \frac{P_{out}}{P_{in}} \times 100\% \quad (4)$$

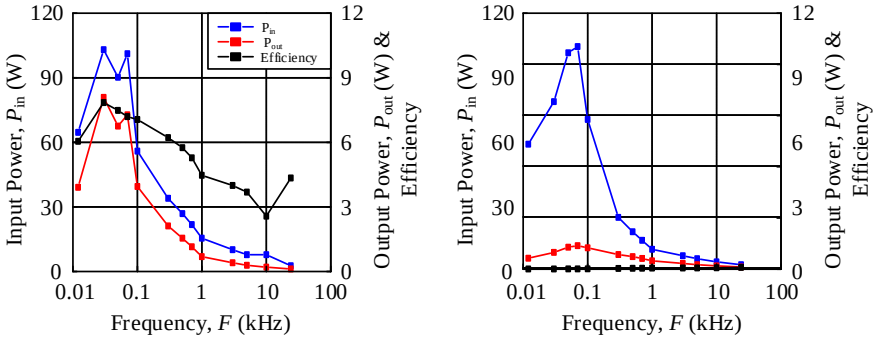

(a) No gap **(b) 5 mm**

Fig. 8. On-load power and efficiency.

5. Conclusions

For this project, able to construct the structure of wireless power transfer. From fabricating the WPT module, that uses different parameters in both the primary coil and secondary coil. The secondary coil has greater parameters than the primary coil in term of turns and layers to achieve the highest output voltage as possible. The experiment results show that the frequency and air gap influence the inductance and the resistance of the module constructed. The frequency and air gap also affect other performances such as voltage, current, and power.

Acknowledgements

The authors would like to thank the Ministry of Education and Universiti Teknikal Malaysia Melaka (UTeM) for providing PJP/2017/FKE/HI12/S01537.

References

1. Vikay Kumar, V.; Niklesh, P.; and Naveen, T. (2011). Wireless power transmission. *International Journal of Engineering Research and Technology* (IJERT), 1(4), 1506-1510.
2. Chopra, S.; and Bauer, P. (2013). Driving range extension of EV with on-road contactless power transfer - A case study. *IEEE Transactions on Industrial Electronics*, 60(1), 329-338.
3. Qiu, C.; Chau, K.T.; Liu, C.; and Chan, C.C. (2013). Overview of wireless power transfer for electric vehicle charging. *Proceedings of the World Electric Vehicle Symposium and Exhibition* (EVS27). Barcelona, Spain, 1-9.
4. Mai, R.; Liu, Y.; Li, Y.; Yue, P.; Cao, G.; and He, Z. (2017). An active-rectifier based maximum efficiency tracking method using an additional measurement coil for wireless power transfer. *IEEE Transactions on Power Electronics*, 33(1), 716-728.
5. Phogat, S. (2014). Analysis of single-phase SPWM inverter. *International Journal of Science and Research* (IJSR), 3(8), 1793-1798.
6. Ismail, B.; Taib, S.; Saad, A.R.M.; Isa, M.; and Daut, I. (2006). Development of control circuit for single phase inverter using atmel microcontroller.

Proceedings of the International Conference on Man-Machine Conference. Langkawi, Malaysia, 4 pages.

7. Vujacic, M.; Hammami, M.; Srndovic, M.; and Grandi, G. (2017). Theoretical and experimental investigation of switching ripple in the DC-link voltage of single-phase H-bridge PWM inverters. *Energies*, 10(8), 16 pages.
8. Gopinath, A. (2013). All about transferring power wirelessly. *Electronics for You*, 52-56.